

# WIND TUNNEL WALL BOUNDARY LAYER CONTROL FOR 2D HIGH LIFT WING TESTING

**Fernando Martini Catalano, PhD; Paulo R. Caixeta Jr., MSc**  
**Aircraft Laboratory, Sao Carlos Engineering School-University of Sao Paulo - Brazil**

**Keywords:** *Aerodynamics, Wind tunnel, Two-dimensional testing, High Lift, Suction.*

## Abstract

*Experimental studies have been conducted to evaluate the effectiveness of the technique that consists in applying suction at the wind tunnel working section walls, around the wing model. A special experimental set-up was developed in order to evaluate the spanwise effect of the horseshoe vortex on the wing aerodynamic characteristics and to optimize the suction area and intensity. This set-up consisted of a two-dimensional wing, which could traverse through the porous turntables located at the end plates. Measurements have been performed at a Reynolds number of  $0.2 \times 10^6$ , with and without suction at 18 spanwise stations. The data evaluated were plots of distributions of  $C_p$  vs.  $x/c$  along the semi-span. Results show that this technique minimizes the three-dimensionality of the flow in two-dimensional testing and the results are sensitive to suction area only at the low pressure surface of the wing.*

## 1. Introduction

Two-dimensional testing, especially with a wing with high lift devices, is an important part of the aircraft design process, in which information about wing sections is revealed. The results provided must be precise enough for use in later calculations.

The aim of this research is to develop two-dimensional testing concepts that are not yet in use in Brazil, but are imperative for the design of a new family of aircraft, which uses high lift systems such as slats and flaps. Wind tunnel tests of this kind should guarantee precision and repeatability over the complete

range of incidence angles and configurations. The very low-pressure upper surface of a high lift wing induces a strong vortex formation between wing and wind tunnel wall or splitter plates causing the flow not to be two-dimensional as expected. Wind tunnels around the world commonly use two techniques to reduce the effects of three-dimensionality present in 2-D tests: sidewall suction or blowing. The pressure gradient between a high lift two-dimensional wing and the walls of the working section of a wind tunnel can be minimized through suction or tangential blowing over certain regions on the walls. It is also possible to minimize the interaction of the wall boundary layer and the wing pressure field.

The suction solution is widely used in important research centers. Paschal et al [1] at NASA Langley Research Center, compared the suction technique with the tangential blowing boundary layer control (BLC) system, and concluded that suction could maintain uniform spanwise flow over the model over a wider range of Reynolds numbers than blowing. Valarezo et al [2] used the suction BLC in the Low Turbulence Pressure Tunnel of NASA Langley, in order to study the performance of multi-element airfoils at various Reynolds and Mach numbers. The technique guaranteed good quality two-dimensional flow for the Reynolds numbers tested. The BLC technique was also used in a study on separation control on high lift airfoils (Lin et al, [3]), with the flow rate adjusted based on the information of pressure taps placed along the span. Lin et al [4] also used again the BLC to investigate parametrically a high lift airfoil, in order to enlarge the experimental database on high lift

aerodynamics for later use in computational fluid dynamics (CFD). Rumsey et al [5], tested several endplate suction patterns with different pressure gradients to drive the suction.

In the present work, suction was used to minimize wing/wall interference. Several suction patterns were tested and its effect on wing pressure distribution in a spanwise direction. The technique developed by this work will be applied to the larger Aircraft Laboratory wind tunnel in order to provide a 2-D high lift facility for further studies.

## 2. The Wind Tunnel Facility and the high lift wing model

The Aircraft Laboratory wind tunnel facility is an open circuit low speed wind tunnel with a 0.260 m high, 0.390 m wide and 0.500 m long test section. Splitter plates were designed to reduce the height of the test chamber so that a traverse mechanism could be used in order to positioning the wing pressure tapping within an adequate vertical range. However, the presence of the splitter plates divided the flow in three parts and, with the presence of the airfoil and its wake, an entrainment of the flow between the plates and the wind tunnel walls occurred. This entrainment is caused by the confluent boundary layers produced by the intersection of the wind tunnel wall and splitter plate boundary layers. In effect these confluent boundary layers restricts the flow between the splitter plates and wind tunnel walls. The main consequence of this effect is that the velocity measured ahead of the splitter plates are not equal to that experienced by the model in the center channel. Consequently, the velocity in the center channel between the splitter plates could not be calibrated against the upstream flow quantity. In order to solve this problem, it was decided to design a ‘new’ contraction, as shown in Fig. 1, and transform the splitter plates in to end plates. The advantage of the small “fresh” boundary of the splitter plate was lost but the flow velocity measurement was precise. The dimension ‘b’ presented in results is equal to half of height ( $b = 0.083$  m) of the “new” test section.

Because of the small scale of the experimental set up, it was decided to use a high lift low Reynolds airfoil instead of a typical multi-component wing. Well-designed low Reynolds airfoils can produce lift coefficients exceeding 2, which was considered high enough to produce strong pressure differences between wall and wing. For this work, the Selig 1223 section was chosen, which can produce  $C_{L,max} = 2.2$  at low Reynolds numbers. The model is made completely of carved wood. It has a span of 0.390 m and a chord of 0.150 m with 36 pressure taps, 19 on the upper surface and 17 on the lower surface, as presented in Fig. (2). No pressure taps could be placed at the trailing edge section due to lack of space. The model has an aspect ratio of 1.1 and a blockage ratio range of 2.75 to 6.86. The flow velocity was measured by a pitot-static tube, located 95 mm upstream of the wing model.

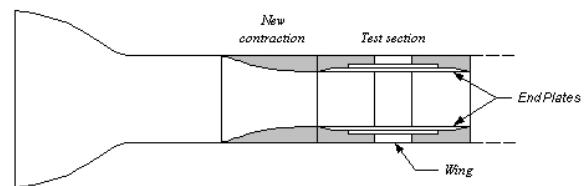


Fig. 1. Cross-sectional sketch of the new contraction and test section.

The cordwise pressure taps are located at the center of the wing but could be moved to different spanwise positions by traversing the wing through the horizontal end plates, as the wing span was greater than the new working section height. The accuracy of the traversing mechanism was  $\pm 0.5$  mm and the reference axis  $Z$  is defined in figure 3. This procedure was very important in the analysis of the flow over the wing surfaces as a fine spanwise distribution of  $C_p$  could be measured. The pressure measurements were performed using a Scanivalve ZOC 33/64 Px X2 with transducer of  $\pm 17,237$  Pa ( $\pm 2.5$  psia) with accuracy of  $\pm 0.08$  % F.S., controlled by a DSM computer data acquisition device. Calibration traceable to the National Institute of Standards and Technology in accordance with MIL-STD-45662A was accomplished on the instrument cited above by

comparison with standards maintained by Scanivalve Corp. The accuracy and stability of all standards maintained by Scanivalve Corp. are traceable to the National Institute of Standards and Technology in Washington DC and Boulder Colorado. A complete record of all work performed is maintained by Scanivalve Corp., is available for inspection upon request.



Fig. 2. Airfoil with pressure tapings positions indicated.

### 2.1 The suction sidewall

1. The suction wall is a porous turntable plate installed in the end plates (or horizontal walls of the new working section). The porous turntable is made of two plates spaced 20mm apart: a perforated steel plate of 20% of porosity and a solid plate forming a plenum chamber where suction was driven by a radial vacuum pump, which was connected to it by a 30 mm diameter tube. There is a lack of information on the wall porosity used in such experiments, so that the porous steel plate used was chosen due to its availability and uniformity. Also, the suction mass flow obtained by the vacuum pump indicated that the porosity should not be less than 10% in order to avoid high-pressure losses. The suction flow rate was controlled by a valve and measured with a calibrated pitot in the pump duct. Figure 3 shows this assembly. Mass flow rate was measured and compared with the working section flow rate to give a suction mass flow ratio. This suction mass flow ratio was defined as:  $\dot{m}_s = \dot{m}_v / \dot{m}_T$  where the subscripts v and T mean vacuum pump and tunnel respectively. The effect of mass-flow rates on the results was investigated. The suction peak of the aerofoil at 10 degrees of incidence with the pressure taps located at the center of the working section was compared for various mass flow rates. The results showed that after  $\dot{m}_s = 0.004$  there was no appreciable change on the suction peak  $C_p$ . Therefore, it was decided to

use  $\dot{m}_s = 0.007$  which was the flow rate for the control valve fully open to avoid pressure losses induced by the valve.

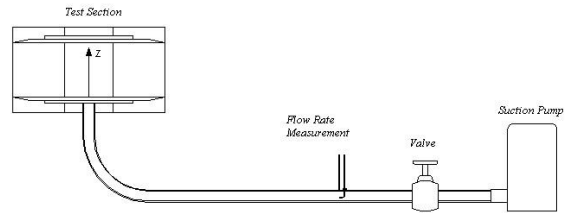


Fig. 3. Assembly of the suction scheme.

To calibrate the pitot, velocity mapping along the pump duct was made. The flow was obtained by integrating the velocities profiles and one point (which had the highest velocity in all profiles measured) was chosen as reference.

The suction area was decided by experiment and the initial size was based on previous work suggestions (Valarezo et al [2] and Paschal et al [1]). Four different porous patterns of suction have been tested, as can be seen on Fig. 4.

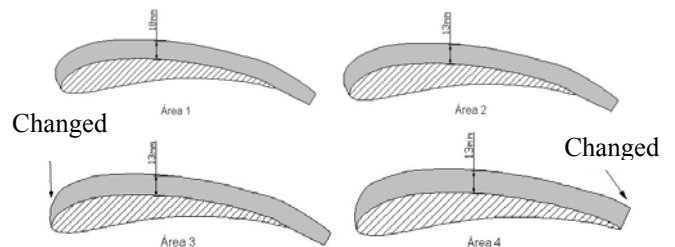


Fig. 4. Cross-sectional sketch of the endplate suction area.

Masking the porous steel plate with a sealing tape was used to achieve the porous patterns. The best porous pattern was determined by testing the four patterns at an angle of attack of  $16^\circ$  where suction peak was high and trailing edge separation was moderate. The Reynolds number was set at 200,000, with a flow rate of 0.007, and model pressure taps line located at stations next to the endplates. The leading edge modification was carried out in an attempt to verify its effect on the location of the suction peak. Comparing the experimental data

with a numerical calculation using a 2-D semi-inverse viscous/inviscid computer program, it was found that a too rounded suction pattern near the leading edge shifts the suction peak forward. Also the fourth modification at the leading edge was carried out due to the effect of this extension on the Kutta condition at the trailing edge making a  $C_p$  value slight higher than one at the stagnation point. Fig. 5 presents the spanwise variation of normal coefficient (CN) in percent of the  $CN_{max}$  calculated by chordwise  $C_p$  integration. Accuracy on  $C_p$  measurements was  $\pm 0.06$ . The porous pattern chosen was area 4 (see Fig. 4) due to the small spanwise variation of CN distribution measured from the wall to the center of the test section. In fact, the porous suction pattern chosen is the most suitable for this wing profile and, the same test procedure should be carried out for a different wing.

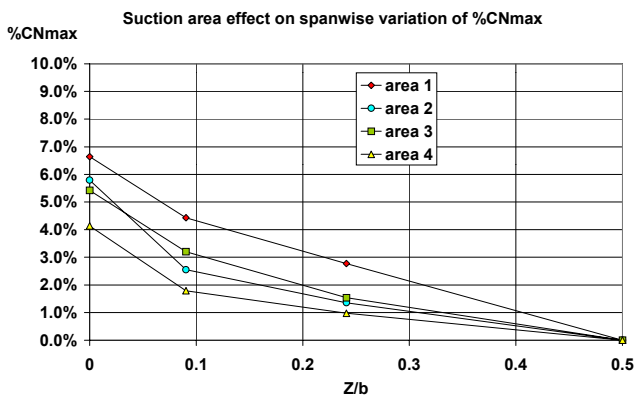


Fig. 5.  $C_p$  at  $1/4$  chord for the endplate patterns.

### 3. Testing procedure

To evaluate the effects of suction over the three-dimensional flow, it was decided to perform the tests, first without suction, with no porous turntables (porous plate covered with a sealant) and then with suction through the area pattern 4. Pressure measurements were made from the center of the test section to the juncture between the wing model and the porous turntable, and from zero angle of attack ( $\alpha$ ) to  $20^\circ$  in steps of  $2^\circ$ .

All the data obtained was reduced to 2-D and 3-D plots with  $C_p$  distribution along the semi-span. In all tests where suction was present, flow rate was 0.007. Uncertainty analysis on measurements was conducted based on Doebelin [6] methodology.

Parameter	Mean Value	Mean Error
T [°C]	2,100E+01	$\pm 5,000E-01$
$\rho$ [kg/m <sup>3</sup> ]	1,102E+00	$\pm 1,880E-03$
$\mu$ [Ns/m <sup>2</sup> ]	1,790E-05	$\pm 2,310E-08$
$P_{d\text{ betz}}$ [mmH <sub>2</sub> O]	1,825E+01	$\pm 1,000E-01$
$V_t$ [m/s]	2,177E+01	$\pm 4,037E-01$
Re	1,957E+05	$\pm 3,880E+03$
$V_s$ [m/s]	1,801E+01	$\pm 5,170E-02$
Q [m <sup>3</sup> /s]	1,175E-02	$\pm 8,495E-04$
$C_p$	xxx	$\pm 6,299E-02$

### 4. Results and Discussion

The tests were performed at a chord based Reynolds number of 200,000. The 2-D plots show the distribution of  $C_p$  ( $C_p \times X/C$ ) for the various spanwise positions, as also do the 3-D plots. The 3-D plots show only the upper surface  $C_p$  distributions where both three-dimensionality and suction effect are more significant; therefore, the phenomenon is better elucidated. Only the plots for  $\alpha = 0^\circ, 10^\circ$  and  $16^\circ$  are presented in this section. In the surface plots the wind tunnel wall is represented on the left side, and the right side is the center of the working section. Flow direction is from page to reader.

Large adverse pressure gradients induced by the high-lift airfoil nearby cause the tunnel side-wall boundary layer to separate, resulting in the loss of uniform spanwise (two-dimensional) flow over the model. Once the sidewall boundary layer separates, a three-dimensional flow pattern is formed in the juncture between the airfoil upper surface and the tunnel sidewall. This three-dimensional flow



field contaminates the flow over the low aspect ratio models, resulting in reduced lift. The reduction in lift could be noted in all results as shown in the followings figures by the reduced upper section suction for the cases with sidewall suction off.

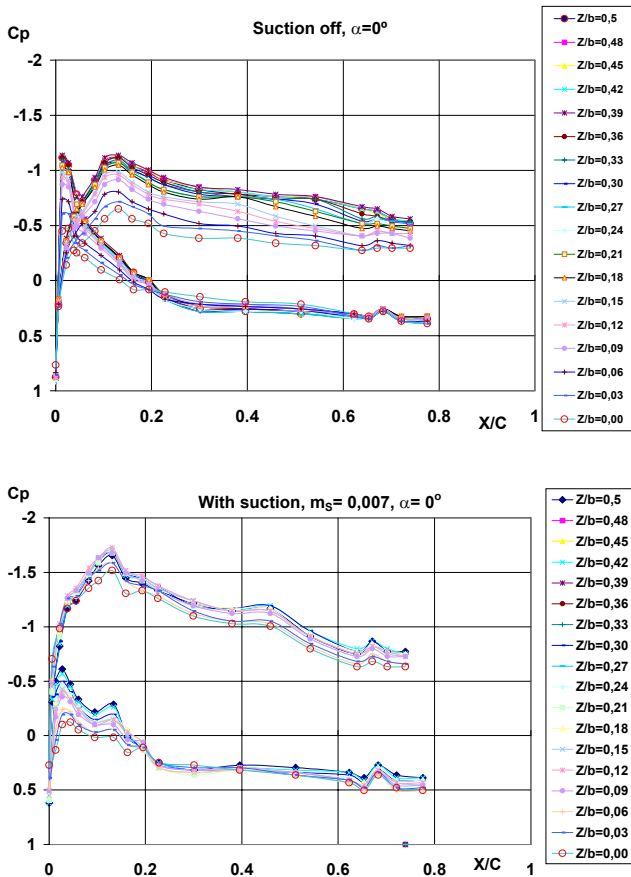


Fig. 6. Comparison of plots  $C_p \times X/C$  at  $\alpha = 0^\circ$  without suction (above) and with suction (right above).

The three-dimensionality of the spanwise pressure distribution can be seen from Figs. 6 to 11 with suction off, as upper surface pressure distribution increases towards the wind tunnel wall. Also, for a high lift airfoil those effects are present in the entire incidence range including (not tested) the zero lift incidence angle. At zero lift a highly cambered wing profile produces strong suction at the bottom surface of the leading edge region inducing the formation of a vortex due to the interaction of this pressure field and the wind tunnel wall boundary layer.

The low-pressure field at the bottom surface is only present at zero and negative incidence angles, so it is important that a special care should be taken to avoid this effect when testing at these incidences. Fig. 6 shows that the wall suction modifies the stagnation region and increases overall upper surface suction but still some flow three-dimensionality at the front part of the bottom surface as no sidewall suction was performed at that part.

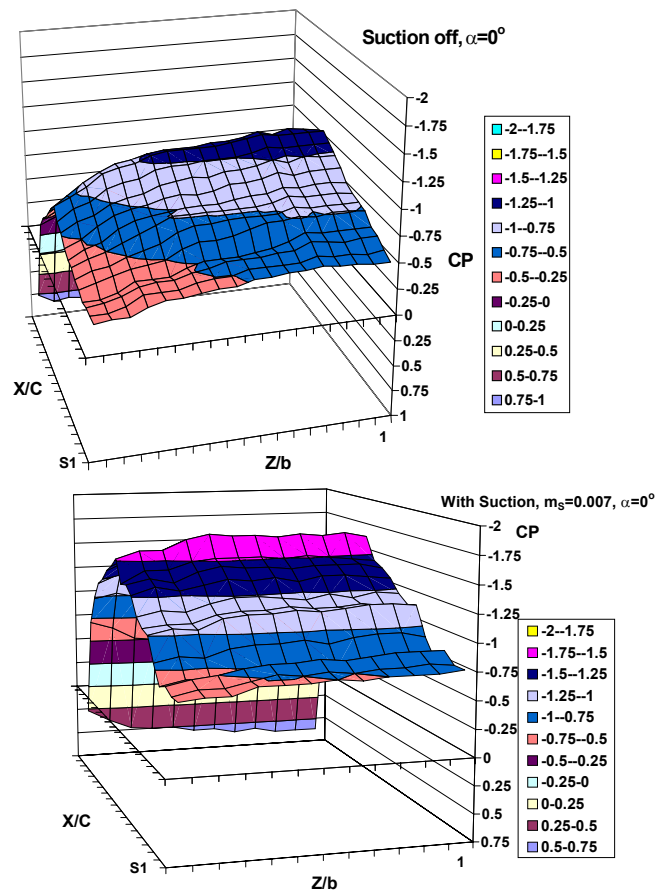


Fig. 7. Surface plots of  $C_p$  distribution without suction (left) and with suction (right) at  $\alpha = 0^\circ$ .

The flow three-dimensionality at the bottom surface is very weak for all the incidences larger than zero although the "new" pressure field at upper surface due to wall suction has a modified stagnation line as can be seen in Figs. 8 and 10. Low Reynolds associated phenomena such as laminar separation bubble and reattachment slightly changes positions under sidewall

suction, as it can be seen at Figs. 8 and 10 for  $\alpha=10^\circ$  and  $\alpha=16^\circ$  at 20% $c$  and 15% $c$  respectively. The difficulty of positioning pressure tapping at the trailing edge made the interpretation of the effect of wall suction on the turbulent separation not conclusive for this testing. However, results in previous works (Paschal et al, [1] and Lin et al, [3]) indicate that flow two-dimensionality in this region have been improved upon sidewall suction.

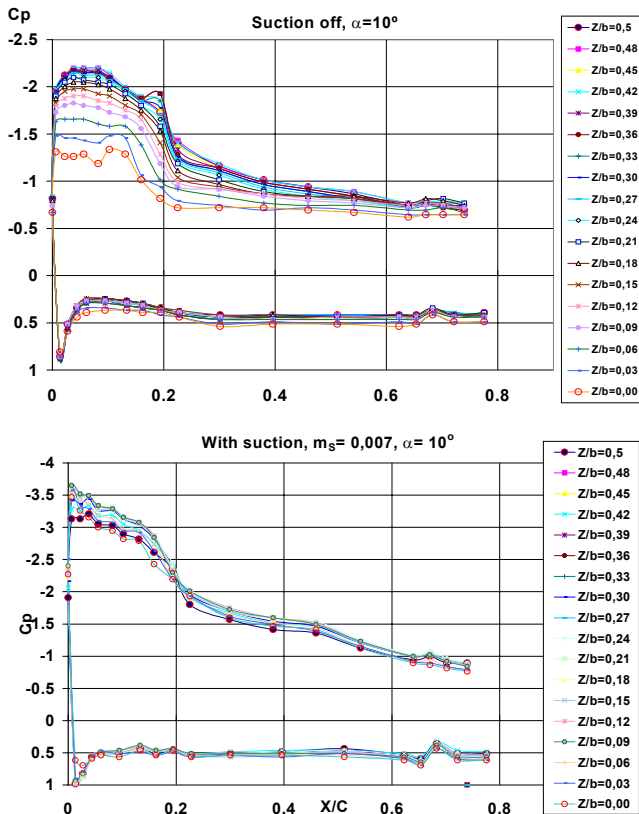


Fig. 8. Comparison of plots  $C_p \times X/C$  at  $\alpha = 10^\circ$  without suction (above) and with suction (right above).

For all the incidence angles tested there was a great improvement of flow two-dimensionality with sidewall suction but the ideal sidewall porous patterns should be experimentally determinate for different airfoil section. In order to indicate if the suction flow and porous patterns are correct, a comparison of the experimental results with numerical calculations was performed. A two-dimensional semi-inverse viscous program was used to carry out the calculations. The evaluations were made by

comparing both pressure distributions and normal force coefficients (CN). The model normal force coefficients were calculated by both chordwise and spanwise integration of CP distribution. The inexistent pressure distribution at the trailing edge was simulated repeating the last CPs for the  $X/c$  0.8 and 0.9 and equaling to zero at  $X/c = 1$ .

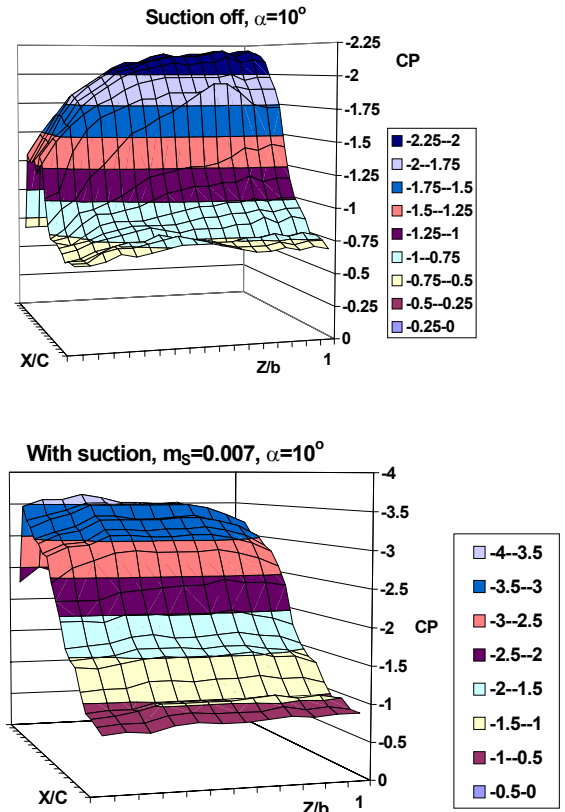


Fig. 9. Surface plots of  $C_p$  distribution without suction (left) and with suction (right) at  $\alpha = 10^\circ$ .

From Fig. 12 it is possible to note that the experimental results utilizing the suction system agree well with the theoretical curve for most of incidence angle tested. However, some important discrepancies occur at the  $CN_{max}$  region, the theoretical results showed  $CN_{max}$  at  $\alpha = 16^\circ$  and experiments at  $\alpha = 18^\circ$ . These results could indicate that porous area and suction rate is in excess in both front and rear parts of the aerofoil upper surface. This supposition may be confirmed with the discrepancies of CP distribution of Figs 13 and

14 up to 60%  $c$  and after 40% $c$  at incidence angles  $\alpha = 0^\circ$  and  $\alpha = 16^\circ$  respectively. Also, it is possible to see from Fig. 13 and Fig. 14 that the excess of suction at front part of the airfoil changes upwash angle through the span especially for low and moderate incidences.

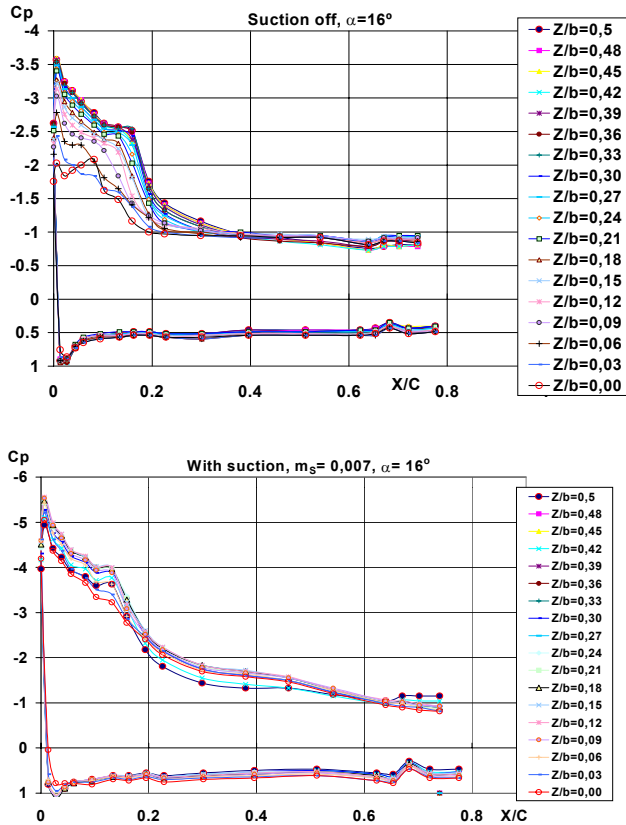


Fig. 10. Comparison of plots  $C_p \times X/C$  at  $\alpha = 16^\circ$  without suction (above) and with suction (right above)

Despite the fact there was an excess of suction, two-dimensional flow has been improved for the entire incidence angles tested. The theoretical results were assumed to be close to the real flow, as there was a large difference between suction-off cases and the numerical results.

### 5. Conclusions

The two-dimensional flow field for two-dimensional high-lift wing testing is a key factor for reliable and accurate data. Ideally, the spanwise pressure distributions should indicate equal pressure levels at all spanwise positions so

that a control of the wind tunnel sidewall boundary layer must be performed. This study consisted of an evaluation of the efficiency and the difficulties in controlling the effects of the sidewall boundary layer and airfoil pressure field interaction by inducing suction at the wind tunnel sidewalls.

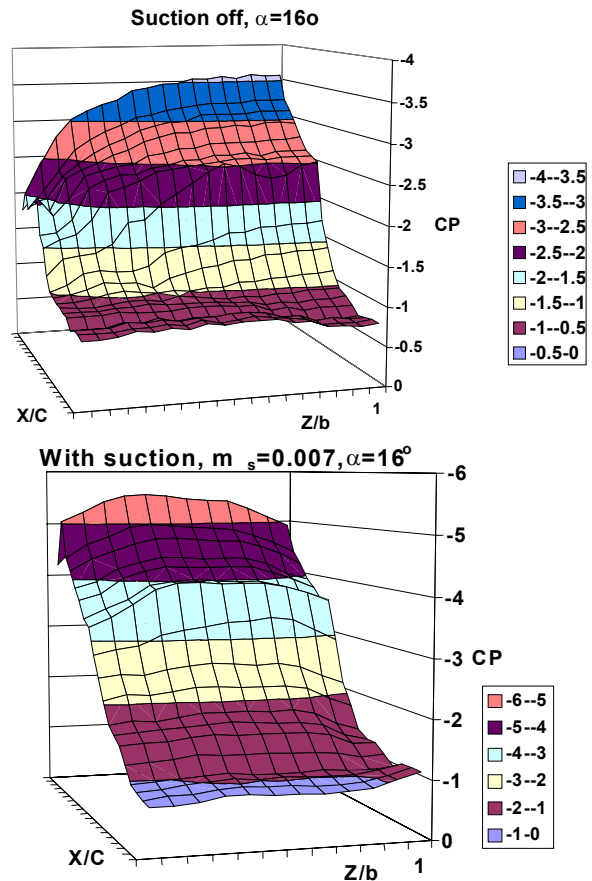


Fig. 11. Surface plots of  $C_p$  distribution without suction (left) and with suction (right) at  $\alpha = 16^\circ$ .

The suction system tested demonstrated the efficacy of this technique as it has completely changed the  $C_p$  distribution over the wingspan. The results of tests with suction show an improvement of two-dimensional flow and high values of  $C_p$ , comparing to the results without suction.

The ideal suction area proved to be a difficult issue as an excess of suction area can modify substantially the spanwise pressure distribution on both lower and upper surfaces of the airfoil. Excess of suction area on the sidewall near the front part of the airfoil can led

to erroneous results for low and moderate incidences, while the excess of suction area at the rear part of the airfoil can increase the suction to values higher than the real flow.

Suction can be applied essentially at the sidewall intersection with the upper surface or only at the rear part of the airfoil, as the lower surface pressure distribution is not highly affected by the sidewall proximity, although some care must be taken when testing high lift wing sections at low incidences. Experimental data was compared with numerical calculations and showed good agreement for most of the incidence range with some discrepancies near the stall.

The whole concept is been adopted to control the wall boundary layer of the 2m<sup>2</sup> low speed wind tunnel of the Aircraft Laboratory. The layout is very similar to the developed in this study. The ceiling and floor turntables have the same plenum chamber with a rectangular porous plate. Suction pumps are installed in both turntables and the air sucked from the working section will return at the fan section. The wing is a 0.5m chord slat/single-flap high lift type with pressure tapping at center chord as well as in three spanwise positions: at 0.3chord, at the slat and at the flap upper surface.

**References**

[1] Paschal, K., Goodman, W., McGhee, R., Walker, B., Wilcox, P. A., Evaluation of tunnel sidewall boundary-layer-control systems for high-lift airfoil testing, *AIAA Paper* 91-3243, 1991.  
 [2] Valarezo, W. O., Dominik, C. J., McGhee, R. J., Multielement airfoil performance due to Reynolds and Mach number variations, *Journal of Aircraft*, Vol. 30, No. 5, pp. 689-694, 1993  
 [3] Lin, J. C., Robinson, S. K., McGhee, R. J., Valarezo, W. O., Separation control on high-lift airfoils via micro-vortex generators, *Journal of Aircraft*, Vol. 31, No. 6, pp. 1317-1323, 1994.  
 [4] Lin, J. C., Dominik, C. J., Parametric investigations of a high-lift airfoil at high Reynolds numbers, *Journal of Aircraft*, Vol. 34, No. 4, pp. 485-491, 1997.  
 [5] Rumsey, C. L., Lee-Rausch, E. M., Watson, R. D., Three-dimensional effects on multi-element high lift computations, *AIAA Paper* 2002-0845, 2002.

[6] Doebelin, E. O., *Measurement systems*, McGraw-Hill Book Company, 1966.

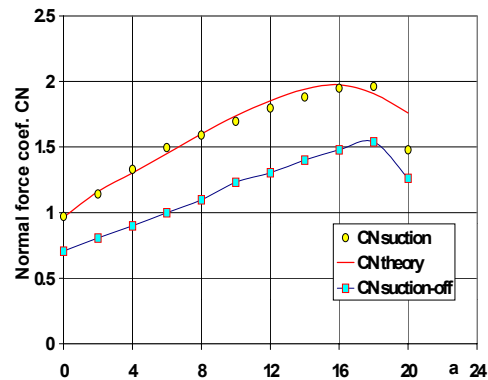


Fig. 12. CNxα from Cp integration.

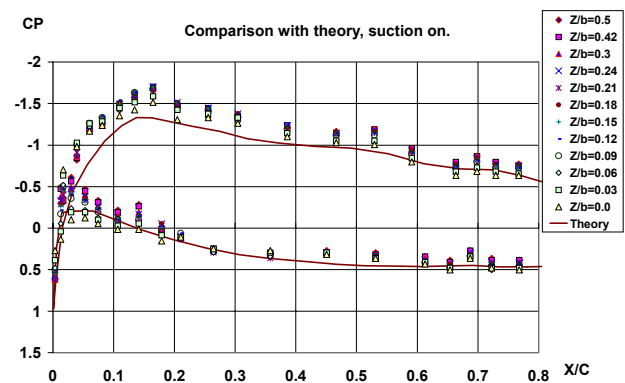


Figure 13. Comparison with theory α=zero.

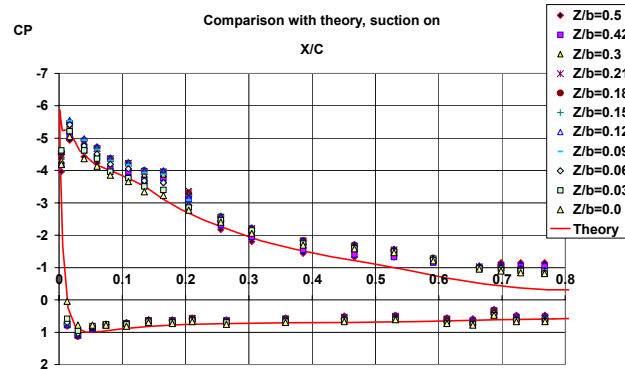


Figure 14. Comparison with theory, α=16°.